Inter-comparison of AIRS temperature and relative humidity profiles with AMMA and DACCIWA radiosonde observations over West Africa

Marian Amoakowaah Osei[1], Leonard K Amekudzi[2], Craig R. Ferguson[3], and Sylvester Kojo Danuor[4]

[1]Kwame Nkrumah University of Science and Technology
[2]Department of Physics, Kwame Nkrumah University of Science and Technology (KNUST), Kumasi-Ghana
[3]Atmospheric Sciences Research Center
[4]University of Science and Technology

November 26, 2022

Abstract

The vertical profiles of temperature and water vapour from the Atmospheric InfraRed Sounder (AIRS) have been validated across various regions of the globe as an effort to provide a substitute for radiosonde observations. But there is a paucity of inter-comparisons over West Africa where local convective processes dominate and RAOBs are limited. This study validates AIRS temperature and relative humidity profiles for selected radiosonde stations in West Africa. Radiosonde data was obtained from the AMMA and DACCIWA campaigns which spanned 2006 - 2008 and June-July 2016 respectively and offered a period of prolonged radiosonde observations in West Africa. AIRS performance was evaluated with the bias and root mean square difference (RMSD) at seven RAOB stations which were grouped into coastal and inland. Evaluation was performed on diurnal and seasonal timescales, cloud screening conditions and derived thunderstorm instability indices. At all timescales, the temperature RMSD was higher than the AIRS accuracy mission goal of ± 1 K. Relative humidity RMSD was satisfactory for the entire troposphere with deviations $< 20\%$ and $< 50\%$ respectively. AIRS retrieval of water vapour under cloudy and cloud-free conditions had no significant difference whereas cloud-free temperature was found to be more accurate. The seasonal evolution of some thunderstorm convective indices were also found to be comparable for AIRS and RAOB. The ability of AIRS to capture the evolution of these indices imply its applicability for determining the thunderstorm probability over West Africa under the Global Challenges Research Fund African Science for Weather Information and Forecasting Techniques project.

Inter-comparison of AIRS temperature and relative humidity profiles with AMMA and DACCIWA radiosonde observations over West Africa

Marian A. Osei [1], Leonard K. Amekudzi[1], Craig R. Ferguson[2], Sylvester Danuor[3]

[1]Meteorology and Climate Science Unit, Physics Department, KNUST, Kumasi-Ghana
[2]Atmospheric Sciences Research Center, University at Albany, State University of New York, Albany, New York
[3]Geophysics Unit, Physics Department, KNUST, Kumasi-Ghana

Key Points:

- Diurnal and seasonal temperature RMSD of AIRS was > 1 °K whereas the RH profiles were more accurate.
- The seasonal AIRS and RAOB derived thunderstorm instability indices were comparable at the stations.
- Capability of monitoring storm evolution with AIRS profiles under the GCRF African SWIFT project.

Corresponding author: Marian Osei, `marianosans92@gmail.com`

Abstract

The vertical profiles of temperature and water vapour from the Atmospheric InfraRed Sounder (AIRS) have been validated across various regions of the globe as an effort to provide a substitute for radiosonde observations. But there is a paucity of inter-comparisons over West Africa where local convective processes dominate and RAOBs are limited. This study validates AIRS temperature and relative humidity profiles for selected radiosonde stations in West Africa. Radiosonde data was obtained from the AMMA and DACCIWA campaigns which spanned 2006 - 2008 and June-July 2016 respectively and offered a period of prolonged radiosonde observations in West Africa. AIRS performance was evaluated with the bias and root mean square difference (RMSD) at seven RAOB stations which were grouped into coastal and inland. Evaluation was performed on diurnal and seasonal timescales, cloud screening conditions and derived thunderstorm instability indices. At all timescales, the temperature RMSD was higher than the AIRS accuracy mission goal of ± 1 °K. Relative humidity RMSD was satisfactory for the entire troposphere with deviations $<$ 20% and $<$ 50% respectively. AIRS retrieval of water vapour under cloudy and cloud-free conditions had no significant difference whereas cloud-free temperature was found to be more accurate. The seasonal evolution of some thunderstorm convective indices were also found to be comparable for AIRS and RAOB. The ability of AIRS to capture the evolution of these indices imply its applicability for determining the thunderstorm probability over West Africa under the Global Challenges Research Fund African Science for Weather Information and Forecasting Techniques project.

1 Introduction

Quantification of atmospheric temperature and water vapour are critical for assessing and improvement of numerical weather and climate prediction models (Diao et al. (2013); Divakarla et al. (2006) and references therein). The initialization process for these models demand the use of denser and homogeneous satellite radiance which must be corrected for cloud contamination. This radiance correction allows for the effective and efficient retrieval of atmospheric profiles such as water vapour, temperature, ozone and other trace gases. Retrieval skill is dependent on sensor accuracy, the atmospheric transmittance functions, cloud clearing and inversion algorithms (Divakarla et al., 2006). The availability and accuracy of observational calibration/validation data, especially observations from radiosondes is critical to the development of robust atmospheric profile retrieval algorithms and products. Water vapour is a particularly important because its presence in the form of clouds can induce either a positive or negative temperature feedback in the climate system based on height of occurrence (e.g.,(Mears et al., 2015)). Therefore understanding and modeling the spatiotemporal variability of atmospheric moisture is essential to weather and climate prediction.

Radiosonde observations (RAOB) offer an adequate platform for the monitoring of the vertical profile of water vapour, temperature, wind, and geopotential height. When assimilated into weather forecast models, RAOBs can enhance the prediction of convective storm evolution in terms of initiation, propagation and decay (Madhulatha et al., 2013; Chen et al., 2014). However the spatial distribution of radiosondes are limited with few launches in the equatorial tropical region that is characterized by strong convective activities (He et al., 2015; Taylor et al., 2017; Parker, 2017). The radiosonde has the advantage of being highly accurate with high vertical resolution (Flores et al., 2013), but the frequency of sonde launches in time and space is low due to the large operational cost (Flores et al., 2013; Bayat & Maleki, 2018). The African Monsoon Multidisciplinary Analysis (AMMA) (Redelsperger et al., 2006) and Dynamics-aerosol-chemistry-cloud interactions in West Africa (DACCIWA)(Knippertz et al., 2017) campaigns in 2006 and 2016 respectively mark years in which RAOBs are available for West Africa.

With advances in remote sensing, sounders aboard satellites offer alternate sources for the acquisition of RAOB-like vertical profiles.. The majority of these validation studies have focused on inter-comparing the retrievals from satellite-based platforms with corresponding collocated radiosonde measurements. A well-known sensor is the Atmospheric Infrared Sounder (AIRS) aboard NASA's Earth Observing System (EOS) Aqua satellite (Aumann et al., 2003). AIRS was constructed to provide atmospheric temperature profiles to a root mean square difference (RMSD) of 1 °K for every 1 km tropospheric layer and 1 °K for every 4 km stratospheric layer up to an altitude of 40 km (Olsen et al., 2017). The corresponding humidity RMSD of the sensor is of order 20% in 2 km layers in the lower troposphere and approximately 50% in the upper troposphere (Susskind et al., 2003; Susskind, 2006). These error estimates are considered to be applicable for scenes of up to 80% effective cloud cover (Susskind, 2007). According to McMillin et al. (2007) (and see references therein), the AIRS instrument has provided a set of unique datasets by which to validate climate and weather models and analyse the global distribution of water vapour and ice supersaturation. AIRS temperature and water vapour datasets have also been evaluated to improve parameterisation of sub-grid scale models (Quaas, 2012) and to understand regional climatology, including land-atmosphere coupling (Ferguson & Wood, 2010, 2011).

Currently, there is a rigorous ongoing AIRS validation efforts using various ground truths across the world, Iran (Bayat & Maleki, 2018), India (Prasad & Singh, 2009; Singh et al., 2017), Antarctica (Boylan et al., 2015) and continental United States (Ferguson & Wood, 2010; McMillin et al., 2007). The studies also provide information on performance improvements of recent AIRS version releases over earlier releases (Milstein & Blackwell, 2016). Most of these studies observed a good agreement between AIRS and RAOB profiles with an overall accuracy within mission-specified accuracy bounds (Xuebao et al., 2005; Milstein & Blackwell, 2016; Prasad & Singh, 2009). Bayat and Maleki (2018) validated AIRS derived precipitable water vapour profiles with a ground-based sun photometer measurements and obtained an acceptable agreement with a 93% coefficient of determination. Seasonal analysis over Iran showed higher dry biases of the precipitable water vapour during spring with lower values in the winter. Over India, Singh et al. (2017) found that AIRS and the Indian National Satellite (INSAT-3D) agree comparatively well with RAOB observations at the lower and upper troposphere but quickly degrades in the middle troposphere probably due to improper bias correction coefficients used for brightness temperature. Their findings observed the influence of surface emissivity on the AIRS profile retrievals which resulted in larger errors over land and in dry atmosphere. Divakarla et al. (2006) also observed a decreased performance of AIRS temperature and water vapour profiles relative to the Advanced TIROS Operational Vertical Sounder (ATOVS) (Reale et al., 2008) retrievals and the National Center for Environmental Prediction Global Forecasting System (NCEP_GFS) and European Center for Medium Range Forecast (ECMWF) forecast profiles over land measurements which exhibited a seasonal and annual variability that correlates with changes in CO_2 concentrations. However, the overall agreement was satisfactory for both land and sea surface categories. Furthermore, AIRS was merged with the Microwave Limb Sounder (MLS) temperature and water vapour records to successfully study the inter-annual variability of these parameters over tropical Pacific (Liang et al., 2011). Their findings revealed the spatial and seasonal distribution of temperature and humidity to be located over the deep convection zone of the tropical western Pacific whereas subsidence dominates at the tropical central Pacific. Based on these datasets, the authors (Liang et al., 2011) were able to observe and link the inter-annual variability of major tele-connections such as the El Nino Southern Oscillation (ENSO), Quasi-Biennial Oscillation (QBO). To date, there have been no dedicated analysis of AIRS retrieval performance over West Africa. For example, Ferguson and Wood (2011) could only utilise four radiosonde observations stations from the AMMA project into the validation section (AIRS versus radiosonde) of their land-atmosphere coupling study.

Our study inter-compares AIRS vertical profiles of temperature and relative humidity with AMMA and DACCIWA radiosonde observations at some selected West African stations for which there are sufficient data matchups. For context, AIRS retrieval skill is compared against that of NCEP_R2 at the same sites. Notably, NCEP-R2 does not assimilate AIRS, as do more modern atmospheric reanalyses, but does assimilate RAOBs. Results from this study will give a first hand confidence in the use of the AIRS datasets for the profiling of temperature and relative humidity that exist in a pre-convective environment for thunderstorm initiation. It is also in accordance with the Global Challenges Research Fund (GCRF) African Science for Weather Information and Forecasting Techniques (SWIFT) project which seeks to develop a sustainable research capability in tropical weather forecasting. The remaining part of the paper is structured into three sections which includes the methodology in Section 2, results and discussions in Section 3 and finally the conclusion in Section 4.

2 Methodology

2.1 Radiosonde Observations over West Africa

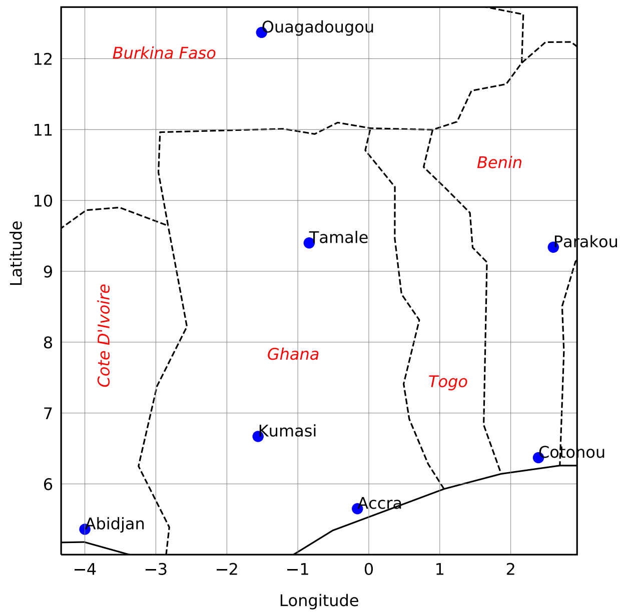

Figure 1. Spatial locations of radiosonde soundings in blue filled circles. Kumasi and Accra are DACCIWA sites while the remaining are AMMA sounding sites. Country of which station sounding was launched is in red italised.

RAOB of temperature and relative humidity profiles were obtained from AMMA (`http://database.amma-international.org/`) and DACCIWA (`http://baobab.sedoo.fr/DACCIWA/` for the period of January 1 2006 to December 31 2008 and June 1 to July 31st 2016, with locations of RAOB locations are distributed between longitudes 4° W to 2° E and latitudes 5° N to 13° N (see Figure 1). The stations Ougadougou (Burkina Faso), Abidjan (Ivory Coast), Parakou, Cotonou (Benin) and Tamale (Ghana) fall within the AMMA project sites whiles Kumasi and Accra (Ghana) fall under the DACCIWA jurisdiction. Under the SWIFT project, Ghana is a country of prime focus and convective activities from neighbouring countries affect the country's weather and hence, this formed the basis for station selections. The Vaisala sondes RS92 were deployed at Abidjan, Tamale, Kumasi, Accra and Parakou, whiles Cotonou and Ougadougou utilised the MODEM SR2K2 radiosondes. Aside from the measured parameters, the radiosonde also provides other parameters such as dew-point temperature, wind speed, wind direction, upward balloon velocity and altitude at standard pressure levels. A limiting element of the Vaisala RS92 instruments is its negative humidity bias obtained during daytime sounding (see Singh et al. (2017) and references therein) resulting from the absorption of gases by the capacitor in sites which otherwise should have been made available for the absorption of water vapour molecules (McMillin et al., 2007). Nonetheless data originating from these instruments have been bias corrected and quality-controlled with appropriate algorithms by the source bodies before release for research activities.

2.2 AIRS temperature and humidity profiles

The AIRS sensor has been operational aboard the AQUA satellite since September 2002 with a nadir polar orbiting mode. It is a cross-track scanning sounder, hyper-spectral resolved, sun-synchronous and a twice daily global scan with an equator overpass at 1:30 am and 1:30 pm for descending and ascending orbits respectively. The sounder provides comprehensive information on the vertical thermodynamic structure of the atmosphere by viewing in 2378 channels along with four visible and near-infrared channels (Olsen et al., 2017; Singh et al., 2017). It as well retrieves infrared and microwave surface emissivity as a function of frequency, total ozone and cloud parameters (Divakarla et al., 2006). The AIRS IR-Only level 3 standard retrieval (AIRS3STD) version 6 algorithm 0.31.0 profiles of temperature and relative humidity has been used for the present study. These products were obtained at a $1^{\circ}\times1^{\circ}$ grid at twice daily temporal resolution. The air temperature were extracted from 11 standard pressure levels (925 hPa - 100 hPa) whiles relative humidity was retrieved at 9 water pressure levels of 925 hPa to 200 hPa. The dataset has been quality controlled with appropriate and improved cloud screening algorithms and uncertainty measures as described in Susskind et al. (2003); Susskind (2006, 2007); Susskind et al. (2011). AIRS3STD is derived from Level-2 data products in which the quality control of every parameter field has been flagged as best (0) or good (1) (Olsen, 2016). This ensures that all grids have the highest quality level datasets for each field and pressure level. Since the analysis of the study depended on the correlation between two parameters at different pressure levels, the combined parameter field (TqJoint grids) for both ascending and descending passes as recommended by Olsen (2016) was used. The TqJoint field applies a single, unified quality control criterion for all parameter fields and has flags of either 0 or 1. The AIRS dataset can be accessed at `http://disc.sci.gsfc.nasa.gov/AIRS/data_access.shtml`.

2.3 NCEP_R2 datasets

The NCEP-DOE Reanalysis 2 (herein NCEP_R2) is an improved version of the NCEP Reanalysis 1 project with an updated parameterisation scheme for physical processes such as new shortwave radiation and changes in boundary layer and minor tuning of convective parameterisation (Kanamitsu et al., 2002). The model uses analysis/forecast system to produce data assimilation from past datasets (1979) to present. The Reanalysis data has been subset into four main categories of Pressure, Gaussian Grid, Spectral Coefficient and Surface Data. Temperature and humidity profiles which are of interest to this study was taken at a 4-times daily and $2.5^{\circ}\times2.5^{\circ}$ spatial resolutions. Observational data which are obtained from NCEP_R2 global upper air Global Telecommunication System (GTS) by the National Center for Atmospheric Research (NCAR) are combined with other datasets such as satellite, marine and surface winds to obtain a desired output parameter (Wang et al., 2016). These datasets can be obtained at the NOAA website `https://www.esrl.noaa.gov/psd/`.

2.4 Data Collocation and Statistical Analysis

2.4.1 Data Sampling

To inter-compare the temperature and relative humidity profile datasets from RAOB, AIRS and NCEP_R2, the datasets were first collocated in both space and time. A temporal sampling window of ±3 hours within a spatial radius of 100 km as used by other AIRS validation studies (Divakarla et al., 2006; Milstein & Blackwell, 2016) was applied to extract the RAOB and NCEP_R2 daily profiles. Table 1 shows the number of retrieved samples from the RAOB to AIRS that satisfied the collocation criteria. The NCEP_R2 profiles which passed this criterion were obtained from synoptic times 00 hours (to match with descending pass) and 12 hours (to match with the ascending pass). A total collocated days of profiles for RAOB and NCEP_R2 each for the AMMA and DACCIWA field campaign sites were totaled at 278 (Abidjan), 176 (Cotonou), 43 (Ougadougou), 104 (Parakou), 27 (Tamale), 8 (Kumasi) and 30 (Accra) (see Table 1). It must be noted that, no temporal interpolation was performed on the AIRS or NCEP_R2 data. Since the accurate retrieval of temperature and water vapour profiles by satellites strongly dependent on the land surface emissivity and skin temperature (Ferguson & Wood, 2010; Singh et al., 2017), these stations have been grouped into "coast"(Abidjan, Accra and Cotonou) and "inland" (Kumasi, Tamale, Ougadougou and Parakou) for analyses. All stations are situated below 925 hPa, therefore profile analyses was initialised at this level to 100 hPa for temperature and 200 hPa for relative humidity.

Table 1. Number of samples retrieved from AIRS-RAOB collocations

Station	Ascending overpass	Descending overpass	Dry Season (December-February)	Wet Season (March-November)
Abidjan	30	248	91	187
Accra	18	12	-	30
Cotonou	58	118	56	120
Kumasi	5	3	-	8
Parakou	18	86	7	97
Tamale	14	13	3	24
Ougadougou	12	31	5	38

2.4.2 Temperature and humidity profile statistics

Equation 1 and 2 with units of °K was used to evaluate the temperature profiles at each pressure level of AIRS and NCEP_R2:

$$Bias = \frac{1}{N}\sum_{i=1}^{N}(T_{DATA} - T_{RAOB}) \tag{1}$$

$$RMSD = \sqrt{\frac{1}{N}\sum_{i=1}^{N}(T_{DATA} - T_{RAOB})^2} \tag{2}$$

The bias and RMSD for calculating water vapour errors were normalised to account for the vertical and temporal variability of water vapour in the atmosphere (Equations 3 and 4) as implemented in Singh et al. (2017). Units of the normalised bias and RMSD for relative humidity is given in percentage (%).

$$Bias_{norm} = \frac{\frac{1}{N}\sum_{i=1}^{N}(RH_{DATA} - RH_{RAOB})}{\frac{1}{N}\sum_{i=1}^{N} RH_{RAOB}} \times 100 \tag{3}$$

$$RMSD_{norm} = \frac{\sqrt{\frac{1}{N}\sum_{i=1}^{N}(RH_{DATA} - RH_{RAOB})^2}}{\frac{1}{N}\sum_{i=1}^{N} RH_{RAOB}} \times 100 \tag{4}$$

where N is the number of collocated temperature or relative humidity profiles for each pressure level, T_{DATA} is the AIRS or NCEP_R2 temperature profile, T_{RAOB} correspond to the radiosonde temperature observations, RH_{DATA} is the AIRS or NCEP_R2 relative humidity profile, RH_{RAOB} imply the radiosonde relative humidity retrievals, RMSD and $RMSD_{norm}$ represent the root mean square difference and normalised root mean square difference derived for the pressure levels respectively.

2.4.3 Thunderstorm convective indices

The AIRS and NCEP_R2 temperature and relative humidity profiles were used to derive three stability indices that affect the evolution of severe and non-severe (Peppler, 1988) thunderstorm occurrences. The derived indices were then used to compare with derived indices of the radiosonde at these observation stations on the seasonal timescale. The indices include the George's K-Index, Total Totals Index and the Humidity Index.
George's K-Index (George, 1960), given by Equation 5 gives a measure of the thickness of low-level and mid-level tropospheric moisture content (Peppler, 1988). Higher values usually >20 °C is indicative of higher probabilities for the occurrence of showers and thunderstorms.

$$K = (T_{850} - T_{500}) + Td_{850} - (T_{700} - Td_{700}) \tag{5}$$

The Total Totals (TT) Index (Miller, 1975)(Equation 6) is a severe thunderstorm indicator which shows the static stability between the 850hPa and 500 hPa levels (Peppler, 1988). It is the sum of vertical totals ($T_{850} - T_{500}$) and cross totals ($Td_{850} - T_{500}$) of temperature and dewpoint temperature. The likelihood of showers and thunderstorms increase as TT index becomes ≥30 °C.

$$TT = T_{850} + Td_{850} - 2T_{500} \tag{6}$$

The Humidity (H) Index given in Equation 7 assesses the extent of saturation at given pressure levels [(Jacovides & Yonetani, 1990; Marinaki et al., 2006) and references therein]. A significant threshold for thunderstorm occurrence should usually be less or equal to 30 °C.

$$HI = (T - Td)_{850} + (T - Td)_{700} + (T - Td)_{500} \tag{7}$$

In all cases, where T and Td are the temperature and dewpoint temperatures in degree Celsius at the reference pressure levels.

2.4.4 Cloud/Cloud-Free Analysis

To further check the strength of the AIRS temperature and relative humidity profiles over the stations, the data was also extracted into days of cloudy conditions and cloud-free conditions. A day is said to be cloud-free if the cloud-fraction is ≤ 0.4. The dataset of which cloud and cloud-free days were extracted for the corresponding radiosonde observations was from the AIRS3STD cloud fraction which is available from `http://disc.sci.gsfc.nasa.gov/AIRS/data\_products.shtml`. Prior to this, lower thresholds less than the stipulated was used but it was observed that, either the collocated criteria was not satisfied, or all radiosonde launch were on days of cloud fraction > 0.4.

3 Results and Discussion

3.1 Diurnal analysis of AIRS temperature and relative humidity

Figure 2 shows the diurnal bias and RMSD for the vertical profile of temperature and relative humidity according to zonal classification. A total of 474 and 182 collocations were found for coast and inland regions respectively. The temperature profile for all passes and locations observed a predominant cold and low biases from the lower to upper troposphere. The biases (Figure 2a) were also found to be increasing with altitude with a sharp inversion observed at the coast (ascending and descending) and inland (ascending). An inversion at the inland for the descending pass is however observed at the 300 hPa pressure level. At the inland stations, the bias between AIRS and RAOB temperature profiles was found to be reduced during daytime passes than the night with an overall pressure level difference about 0.33 °K. In addition this daytime performance inland is also lower than the coastal daytime biases. There were no significant differences between the ascending and descending passes at the coast as was observed inland. Although the biases show AIRS temperature to be constantly underestimated with the RAOB, the retrievals are better at the coast (mean difference) than inland regions. The temperature RMSD profile is shown in Figure 2b with the broken vertical line denoting the AIRS mission temperature accuracy goal of ±1 °K. It can be observed that all over-passes were unable to meet this 1 °K goal with the descending pass of the inland region obtaining between a 4 - 5 °K temperature RMSD. The low bias obtained at the inland ascending pass (Figure 2a) is reflected in the corresponding low RMSD temperature profile (Figure 2b). However the ascending pass for inland also reveals a higher RMSD at the near surface (925 hPa) level denoting the inability of AIRS to retrieve the temperature at this level. On the other hand, at the coast, the 1 °K RMSD is achieved only at the 200 hPa and 300 hPa levels in the ascending pass. The diurnal coastal RMSD ranged between 1 - 4 °K with better retrievals during the ascending than descending pass. Above 200 hPa, there is a degradation in the RMSD for all locations and passes. In general, the daytime analyses show that AIRS temperature profiles for the inland stations have a lower RMSD than the coastal stations, whereas the opposite holds at night. This can be attributed to the diurnal effect of sea and night breezes which is stronger at the coast than inland and invariable affect the temperature retrievals by AIRS.

The statistical analyses for the diurnal retrievals of relative humidity is shown in Figure 2c (bias) and d (RMSD). The RH bias is observed to be warm and positive at the coast and inland for all passes except the inland nighttime retrievals. Biases are also observed to be lower for the coastal region with a near overlap at the surface (925 hPa) to mid-troposphere (500 hPa), above which there exists a relatively small deviation in both day and night passes. AIRS over-estimates the RH for the inland stations during the day and underestimates at night due to the poor retrieval of nighttime temperatures as found in Figure 2 a and b. The inland profile for the day increases steadily from 10% - 25% at the lower to upper troposphere (925 hPa to 200 hPa) as compared to the decreasing trend (<-10%) observed for the nighttime pass. The RH accuracy goal for AIRS is about ±15% - 20% (Susskind, 2006; Divakarla et al., 2006) for the lower to mid-troposphere and better than 50% (Olsen et al., 2017) for the upper troposphere. Unlike the temperature, the relative humidity RMSD (see Figure 2d) was found to be within the AIRS accuracy goal with a slight exceedance (about 3%) at the 200 hPa level for the inland and coastal ascending pass. Although the accuracy goal for the lower to middle troposphere was not satisfied for both locations in the ascending pass, nonetheless the RMSD is quite acceptable. The RMSD for the descending pass was observed to lower than 15% with the upper troposphere ranging between 16 - 20%. Deviations between the coastal and inland regions were highest below 400 hPa and 500 hPa for the descending and ascending passes respectively. The general underestimation of temperature and over-estimation of relative humidity show the effects of temperature retrievals on the RH by AIRS. Pfahl and Niedermann (2011) state that a strong anti-correlation exists between temperature and relative humidity, arising primarily from convective precipitation that decrease local temperatures due to vertical mixing and insolation reduction from clouds. The existence of an indirect relationship

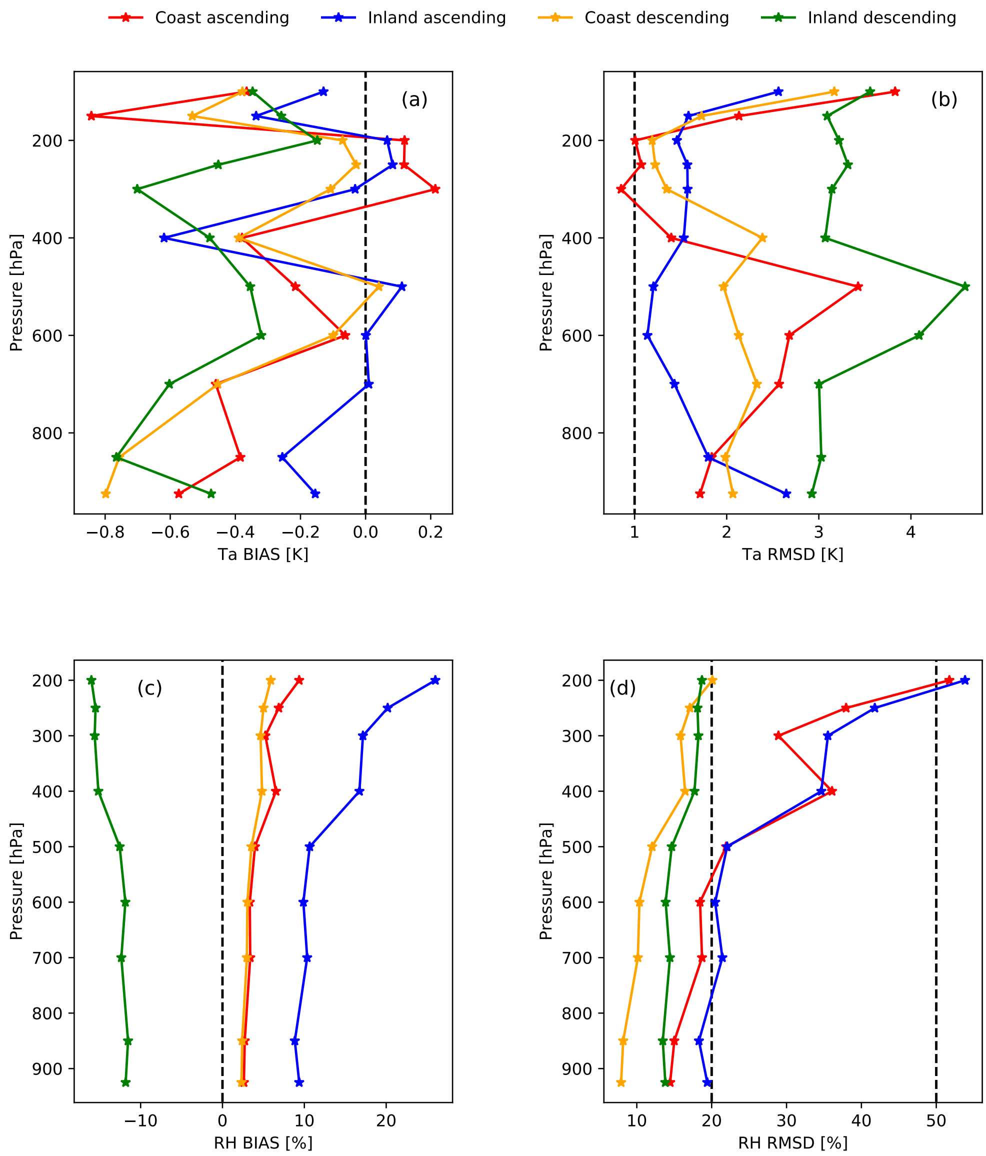

Figure 2. Diurnal retrieval statistics of AIRS for temperature (**a** and **b**) and relative humidity (**c** and **d**) for coastal and inland stations. Broken vertical lines in RMSD represent AIRS accuracy goal for temperature (**b**) and relative humidity (**d**). The first and second vertical lines at 20% and 50% in the RH RMSD shows the accuracy goal for lower and upper troposphere respectively. Recommended bias at broken vertical line 0 °K.

between temperature and relative humidity mean that the relatively lower temperatures (dry bias profile) retrieved by the sensor is translated into a warm bias in the corresponding RH profiles.

3.2 Seasonal analysis of AIRS temperature and relative humidity profiles

Figure 3 shows the seasonal vertical temperature and relative humidity profiles for the coast and inland regions. The seasonal analysis consists of a dry and wet with stations such as Abidjan, Accra, Cotonou and Kumasi experience a bi-modal pattern of rainfall with the major rains occurring between March to July and a minor wet season between September to early November (Amekudzi et al., 2015; Baidu et al., 2017; Parker, 2017). The dry season at these stations also occurs from late November to February. Tamale, Parakou and Ougadougou have a uni-modal rainfall pattern occurring between April to October and a dry season from November to March (Amekudzi et al., 2015; Parker, 2017). The locations which have bi-modal rain pattern observes annually a temporal break in the month of August which is termed as the “little dry spell” (Parker, 2017).

From Figure 3a, the temperature bias was found within a -2.5 to 0 °K with a consistent cold

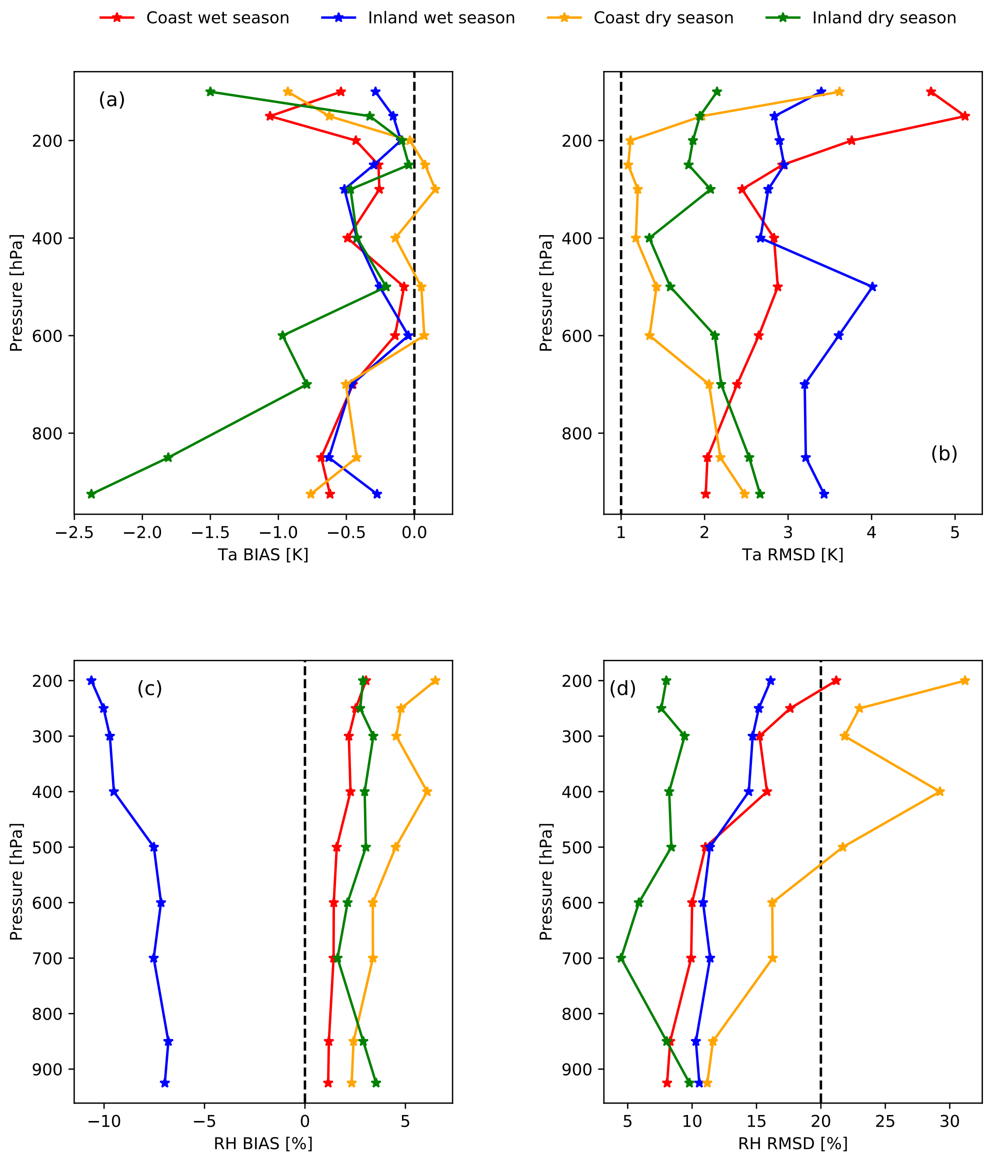

Figure 3. Seasonal statistics of AIRS for temperature (**a** and **b**) and relative humidity (**c** and **d**) for coastal and inland stations. Broken vertical lines in RMSD represent AIRS accuracy goal for temperature (**b**) and relative humidity (**d**). The first and second vertical lines at 20% and 50% in the RH RMSD shows the accuracy goal for lower and upper troposphere respectively. Recommended bias at broken vertical line 0 °K.

bias at all vertical levels. Inland dry season temperatures obtained the highest deviation occurring at the surface to middle troposphere (925 hPa to 500 hPa). The dry season coastal bias was larger above 200 hPa. Between 600 hPa to about 200 hPa, both RAOB temperatures and AIRS retrievals were observed to be similar and accurate for AIRS as the bias was found to be close to zero. Furthermore, AIRS temperature bias and RMSD (see Figure 3a and b) for the dry season are observed to be more accurate than the wet season possibly due to the effect of increasing cloud cover in the wet season that lowers the accuracy of temperature retrievals. According to Ferguson and Wood (2011) increasing cloud cover attenuates the infrared waves for accurate retrievals of temperature by the AIRS sensor. The deviation found at the 925 hPa to 500 hPa for the inland dry season bias is due to higher retrievals from the radiosonde for the season. The coast also obtained smaller biases as compared to the inland stations. The bias at the coast was found to sharply deviate at the 150 hPa level ($\approx$ -1.2 °K) whereas the inland region was quite consistent. The RMSD of the seasonal temperature (Figure 3b), similar to the diurnal temperature RMSD (Figure 2b), failed to meet the AIRS accuracy goal with a spread of 1.5 - 5 °K. The retrieval pass with skill is close to the targeted accuracy was observed in the coastal dry seasonal sample. This can be observed at the 600 hPa to 200 hPa pressure levels where the was a close agreement with the lowest bias between the AIRS and RAOB datasets. In addition, the lower tropospheric (925 hPa to 700 hPa) temperature for the coastal dry season was found to be higher between 2 - 3 °K. For both coastal wet and dry seasons, higher RMSD existed at the upper atmospheric levels with the coastal wet season obtaining a larger deviation. The inland seasons also observed to be accurate than the wet season. In general, the dry season RMSD temperature profiles was found to be lower than the wet season profiles with the coast out-performing the inland stations at all temporal scales.
The bias and RMSD for the relative humidity is shown in Figure 3 c and d. A warm bias (Figure 3c) exists at the coast for both seasons and inland for the dry season only, suggesting an over-estimation of water vapour profiles by the AIRS sensor. On the other hand, the inland wet season is observed to be negatively (cold) biased which can be linked to the occurrence of convection during this season (Prasad & Singh, 2009) and the relatively longer distance traversed by the satellite to retrieve relative humidity inland (McMillin et al., 2007). This cold bias (about 6%) further declined at the upper troposphere. The positive bias was observed between 0 - 5%, which is low and acceptable for a difference between AIRS and RAOB water vapour profiles. At the coast, the wet season although positively biased has the best accuracy (about 1 - 1.5%) as compared to the dry season and inland regions. The RMSD profile (Figure 3d) reveals a satisfactory performance of the AIRS dataset. Tropospheric water vapour profiles at all pressure levels were mostly within 20% and 50% at the coast and inland. Inland dry season AIRS retrievals were observed to be superior with total vertical RMSD less than 10%. The RMSD performance for the inland dry season imply the presence of clear sky conditions which is a major characteristic of the inland stations during this season. Although the bias observed for inland wet season (see Figure 3c), the RMSD is comparable to the coast wet season profile and both were found to be within an acceptable range. The warm bias obtained for the coastal wet season was also found translate into higher RMSD in Figure 3d. In conclusion, the diurnal and seasonal inter-comparisons enhance understanding on the usefulness of AIRS temperature and relative humidity profiles for thunderstorm prediction based on the derivation of instability indices.

3.3 Cloud dependence of AIRS temperature and relative humidity retrieval accuracy

To assess the impact of clouds on the retrieval of temperature and relative humidity by AIRS, the data was separated into days of cloudy retrieval and days of cloud-free retrievals over all overpasses. Only stations Accra, Abidjan, Cotonou and Ougadougou satisfied the cloud and cloud-free (cloud fraction less than 0.4) criteria. The remaining stations, Parakou, Kumasi and Tamale either had no cloud-free days or the collocation window was beyond that stipulated for in this study ($\pm$ 3 hours and a 100 km radius).

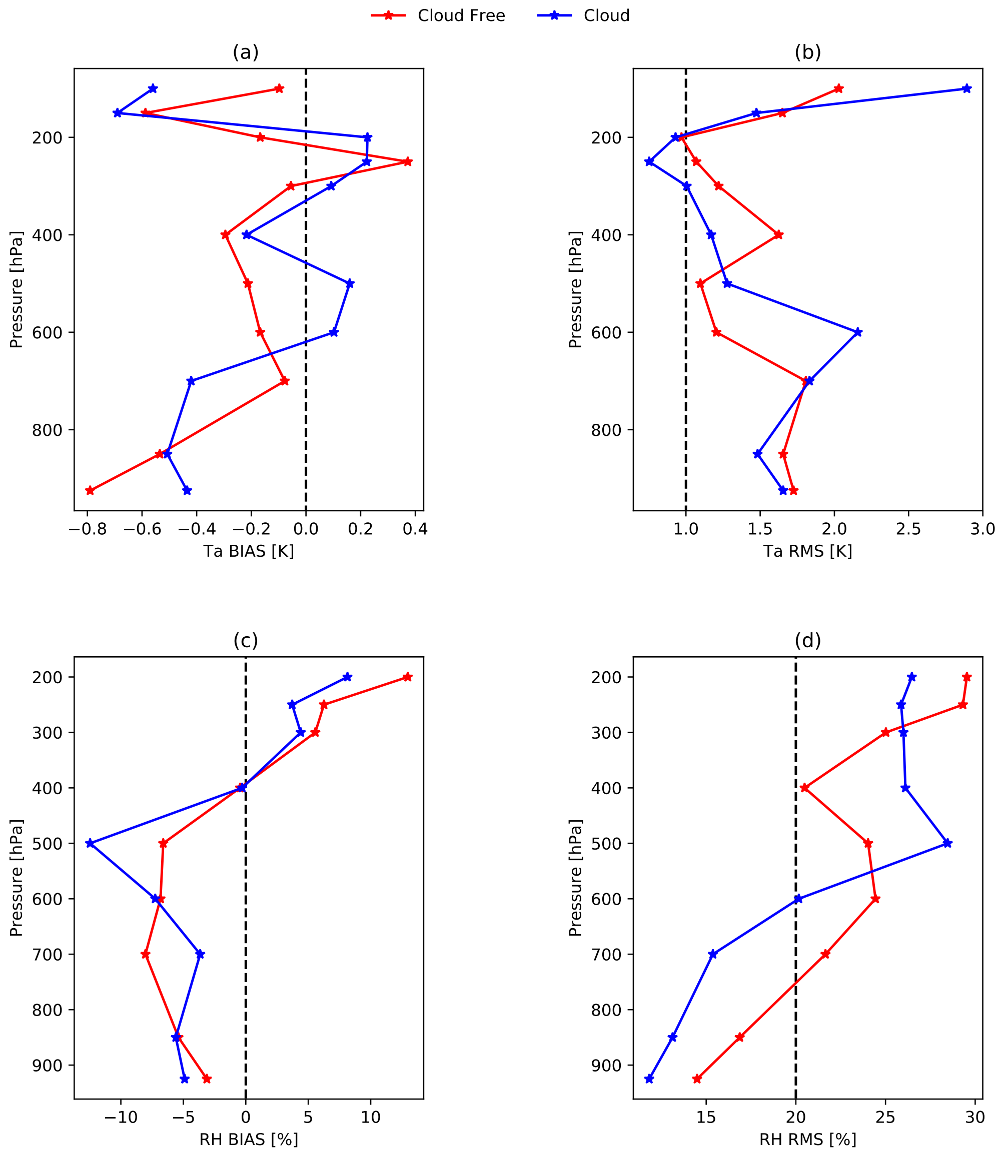

Figure 4. Cloud conditional analyses for all AIRS matchups (ascending and descending overpass) at all stations (see Table 1) for temperature and relative humidity.

The total bias and RMSD profile for the temperature and RH at these stations is shown in Figure 4. The temperature bias (Figure 4a) shows lower bias on cloud days as compared to cloud free days. The bias for both profiles was found to be mostly cold with a warm bias found at the 250 hPa level on cloud free days. On cloudy days, a warm bias was observed at the middle (600 and 500 hPa) and upper (300 to 200 hPa) troposphere. Temperature retrievals at the near surface (Figure 4a) by AIRS was found to be drier on cloud-free days than cloudy days. The RMSD profile shows that the overall performance of AIRS on cloud free days is closer to the mission goal than on cloudy days. There is a higher deviation in both cases at the upper troposphere (150 to 100 hPa) with the largest RMSD found during cloudy days. Upper tropospheric temperature errors on the cloudy days could reach a maximum of 3 °K with a 2 - 2.5 °K on cloud-free occasions. Interestingly, although AIRS cloud-free profile could not meet the accuracy goal at any level, cloudy profile observed a

between 0.5 - 1.0 °K RMSD at the 300 hPa to 200 hPa. This corresponded to the upper tropospheric levels with warm temperature bias (Figure 4a). The alternating RMSD profile also suggests that the accuracy of cloud-free retrievals is better at 700 hPa to 500 hPa and 100 hPa levels whereas cloud retrieval accuracy is better at all other levels.
Figure 4c and d shows the AIRS bias and RMSD for relative humidity on cloud and cloud free days. In general, cold to warm biases are observed to exist on both cloud and cloud free days. Bias in cloud free days is minimal as compared to cloudy conditions. The lower to mid-tropospheric dry bias under cloudy conditions was also observed by Ferguson and Wood (2010) who found a maximum -29% bias in increasing cloud coverage and -15 to -40% by Wong et al. (2015). The cold bias present for both cloud and cloud-free days occurred at the surface to about 500 hPa (Figure 4c). Beyond this level, a warmer bias is observed to reflect an over-estimation of the AIRS profiles especially at the 150 hPa and 100 hPa levels. The effect of clouds on retrievals at the 850 hPa and 500 hPa were found to be negligible as there was an overlap for both scenarios. Overall bias range was within a $\pm$ 10%. On the other hand, RMSD profile (Figure 4d) shows accurate retrievals under cloudy conditions than non-cloudy condition. AIRS accuracy mission goal is satisfied under all occasions for the lower and upper troposphere. Upper tropospheric relative humidity RMSD was observed to be less than 30% for the cloud and cloud-free days with the cloud-free days slightly out-performing the cloudy days. For the lower to middle troposphere, the RMSD for cloudy conditions was observed to be lower than cloud-free days. At the 850 hPa, a higher RMSD exceeding the goal limit of $\leq$ 20%.

3.4 AIRS and NCEP_R2 retrieval skill comparisons

Figure 5 shows the performance of AIRS and NCEP_R2 with RAOB temperature and relative humidity profiles for the coastal and inland regions. To find the overall performance of both AIRS and NCEP_R2, all overpasses of AIRS were merged and compared with the corresponding profiles of NCEP_R2. Cold biases are observed to dominate the coastal AIRS temperature retrievals whereas the inland AIRS temperature profile decreases from warm (below 600 hPa) to cold (above 600 hPa) (see Figure 5a). NCEP_R2 for the coast alternates between cold bias at the surface to mid-troposphere, beyond which a warm bias exists. The inland NCEP_R2 temperature bias profile is also pre-dominantly cold except at the 925 hPa and 250 - 200 hPa pressure levels. Comparing the location biases of AIRS and NCEP_R2 temperature, inland AIRS over-estimates NCEP_R2 profiles at the surface to middle troposphere and under-estimates at the upper troposphere. Alternatively, the coastal performance observes NCEP_R2 to over-estimate the AIRS temperature bias profile at the upper troposphere. The temperature RMSD profile is shown in Figure 5b for AIRS and NCEP_R2. Both AIRS and NCEP_R2 were unable to reach the AIRS accuracy goal except at the 600 hPa and 250 hPa for NCEP_R2 inland statistics. The performance for both datasets was observed to be better for the inland region than the coast. The inland AIRS and NCEP_R2 showed temperature profiles with decreasing RMSD from 3 °K to about 1 °K from the surface to 600 hPa and a significant increasing RMSD from 250 hPa to 150 hPa. The RMSD at the coast was relatively higher with greater deviation within the NCEP_R2 datasets. The highest difference between the coast and inland regions for AIRS and NCEP_R2 occurred from the 850 hPa to 250 hPa levels. Regardless of station, there was a tendency for higher RMSD at the upper troposphere with the maxima occurring in the the NCEP_R2 coastal temperature and the least in the AIRS inland temperature.
The bias and RMSD profile for AIRS/NCEP_R2 relative humidity is observed in Figure 5c and d. Bias (Figure 5c) was found to be in range of -6% to 10% for both datasets. AIRS and NCEP_R2 coastal water vapour is observed to be constantly under-estimated as compared to an over-estimation for the inland. The coastal under-estimation is however observed to be smaller ($\approx$-2% to -3%) than the inland RH over-estimations ($\approx$4% to 6%). Bias was also observed to be increasingly higher (inland) and lower (coast) at the upper levels. In addition, the bias reveals lower values of AIRS at the coast than inland with the reverse being observed in the NCEP_R2 relative humidity profile. The RMSD (Figure 5d) reveal

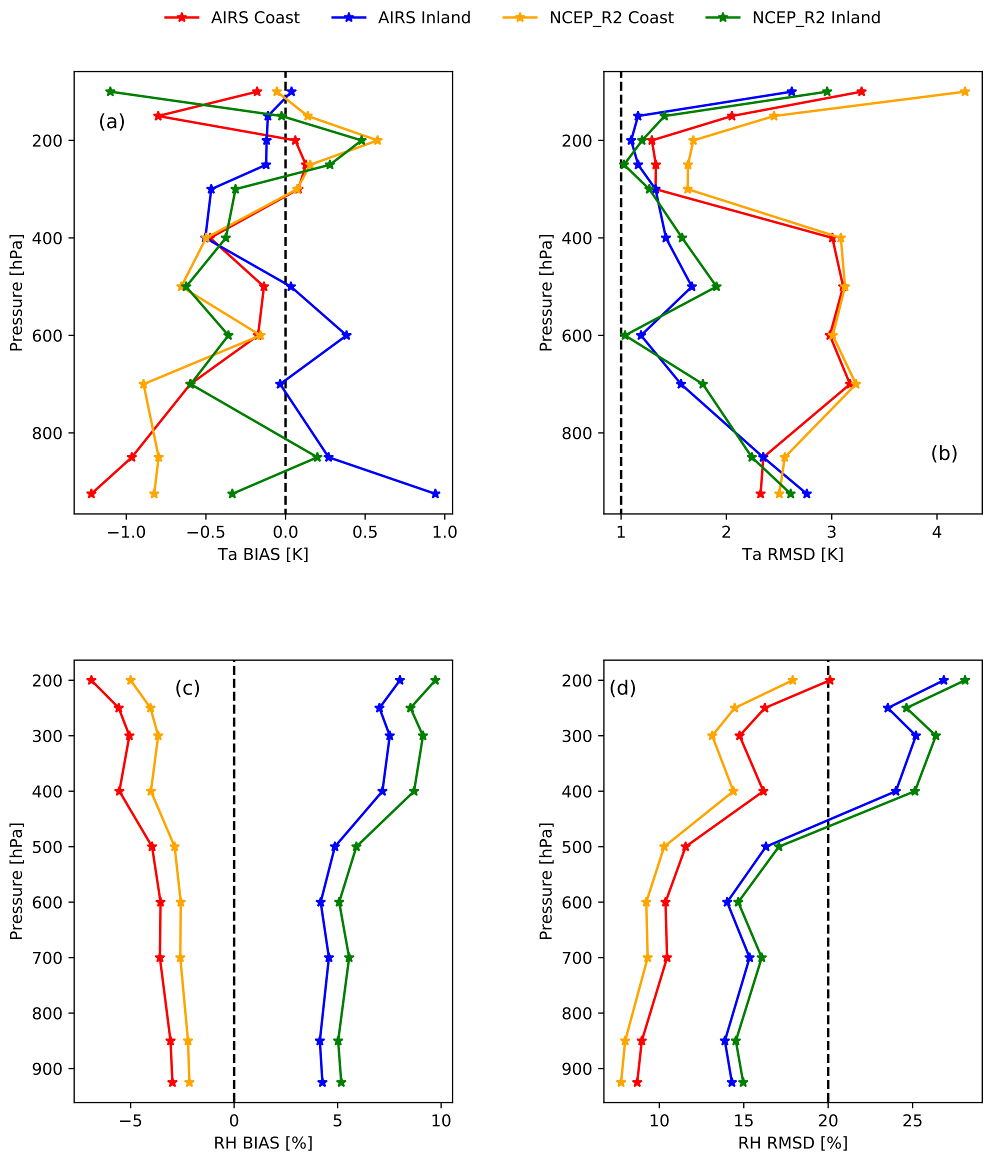

Figure 5. Diurnal uncertainty statistics of AIRS and NCEP_R2 for temperature (**a** and **b**) and relative humidity (**c** and **d**) profiles for coastal and inland stations. Coastal and inland statistics are a merge between the daytime and nighttime datasets. Broken vertical lines in RMSD represent AIRS accuracy goal for temperature (**b**) and relative humidity (**d**). The first and second vertical lines at 20% and 50% in the RH RMSD shows the accuracy goal for lower and upper troposphere respectively. Recommended bias at broken vertical line 0 °K.

the datasets to achieve both lower and upper tropospheric water vapour accuracy goal. As lower biases were obtained over the coast, this is reflected in the higher satisfactory performance in the RMSD (< 20%) for the upper and lower troposphere. Furthermore, the NCEP_R2 is found to give relatively accurate estimates of the tropospheric water vapour content than AIRS along the coast, probably due to the better representation of coastal RAOB information into NCEP_R2 model run. Although the upper tropospheric RMSD was acceptable for both datasets inland, the profile was observed to be sharper from the 500 hPa level as compared to the coast. AIRS is also observed to outperform NCEP_R2 inland than at the coast. In general, the performance of AIRS and NCEP_R2 for RH is acceptable and satisfactory. The satisfactory performance of NCEP_R2 is expected as global RAOB information is incorporated in the estimation of temperature and relative humidity profiles Divakarla et al. (2006). Table 2 is a summary of the AIRS performance at the various atmospheric pressure levels for temperature and relative humidity.

Table 2. Summary of RMSD AIRS-RAOB accuracy for temperature and relative humidity. Values in bold represent atmospheric levels at which RMSD for temperature was atleast closer to the AIRS accuracy goal (1 ±0.5 °K).

Pressure level (hPa)	Temperature RMSD (%)		RH RMSD (%)	
	Coast	Inland	Coast	Inland
925	2.32	2.76	8.68	7.73
850	2.35	2.34	8.96	7.97
700	3.17	1.56	10.45	9.30
600	2.98	**1.18**	10.36	9.22
500	3.10	1.67	11.55	10.28
400	3.00	**1.42**	16.16	14.38
300	**1.32**	**1.32**	14.75	13.13
250	**1.33**	1.67	16.25	14.46
200	**1.29**	**1.09**	20.10	17.89
150	2.05	**1.16**		
100	3.28	2.62		

3.5 Variation of thunderstorm convective indices at the stations

According to Ferguson and Wood (2011), the AIRS sensor has the potential to be used for local convective rainfall prediction based on thunderstorm convective indices. They derived the convective triggering potential and humidity index (from 50 hPa to 150 hPa above ground level) from AIRS temperature and relative humidity profiles and found these indices useful at geographical locations where the predictive power was high. Therefore, our study also evaluated the AIRS and NCEP_R2 derived convective instability indices: K-index, TT index and HI for West Africa against RAOB derived indices. We have evaluated the seasonal biases in AIRS and NCEP derived convective indices here, which in the future, will need to be translated into terms of actual thunderstorm probability and strength for the region. Figure 6 shows the three year (2006-2008) seasonal climatology of the indices for both AIRS and NCEP_R2. The climatology of the indices for both datasets was observed to be similar with NCEP_R2 overestimating slightly at all seasons. The dry season climatology reveals a high probability of convective activities and rain over the southern part of West Africa especially along the coast as compared to inland areas. The Sahelian region which is further northward of West Africa observes low likelihood of rains. Low K-Index are found over the Sudano-Savanna belt with a decreasingly lower negative probability. Furthermore the HI for the dry period elaborates on the effects of sea breeze on the along the coastal areas which results in relatively high humidity and a corresponding low humidity index. Inland low HI is a consequence of the deciduous and semi-deciduous forest which characterises this zone. On the other hand, the dry harmattan winds which engulf the region with the most affected being the Sudano-Savanna zone observes higher than usual humidity index; exceeding two to three times the recommended threshold of $\leq 30°$ C. This observation is captured in both AIRS and NCEP_R2.

The migration of the ITB, evident in the increased convective activities in over West Africa can also be monitored with these thunderstorm convective indices in the wet season. As

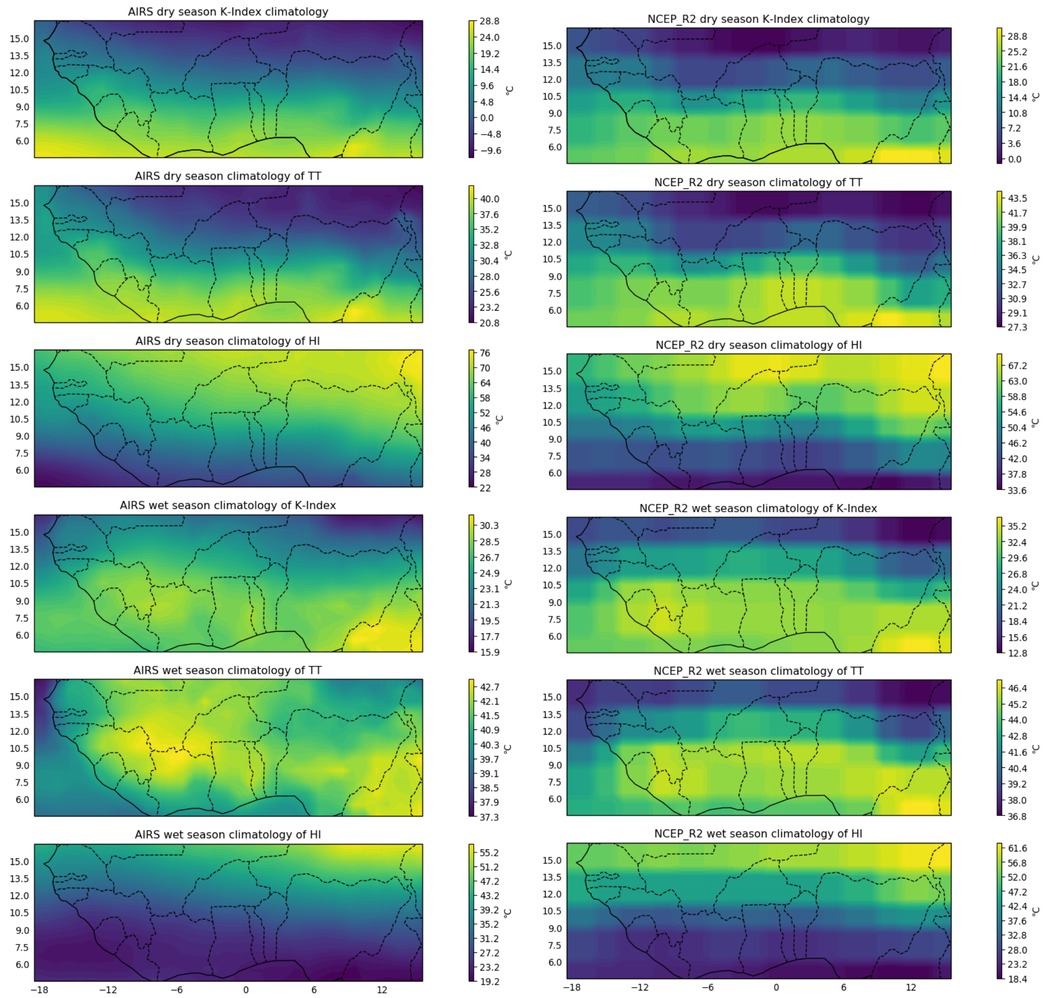

Figure 6. 3 year (2006 - 2008) dry and wet season index climatology from AIRS and NCEP_R2 for the entire West Africa. Dry season include months December, January and February whereas the wet season includes all other months.

can be observed, AIRS shows an under-estimation of K-Index and Total Totals (TT) index probably due to the retrieved relative humidity being lower than the estimates of NCEP_R2 (Figure 6). The HI on the other hand has good correlation for both datasets except at the north-western portion of West Africa which is closer to the Saharan desert. The TT index for NCEP_R2 shows the wet season to have a higher probability of thunderstorm occurrence around latitudes 6° N to 10° N while AIRS shows an isolated maximum concentration of these activities converging over Northern Ivory Coast, North-eastern Guinea, Southern Mali and Burkina Faso (Figure 6). In general, AIRS and NCEP_R2 are able to show the seasonal likelihood of thunderstorm activities over West Africa.

Figure 7 presents the AIRS and NCEP_R2 differences (AIRS-NCEP_R2) for the thunderstorm indices based on the seasonal climatology. Generally, NCEP_R2 is found to over-estimate the occurrence of precipitation in the dry season based on the indices. However, this over-estimation is also found to be lower and reduced in during the wet season. Deviations were highest for the HI in both dry and wet season as compared to the other indices. The dry season K-Index reveals an over-estimation of NCEP_R2 over the entire West African sub-region with AIRS over-estimating off the coast of Liberia and Senegal. This is likely

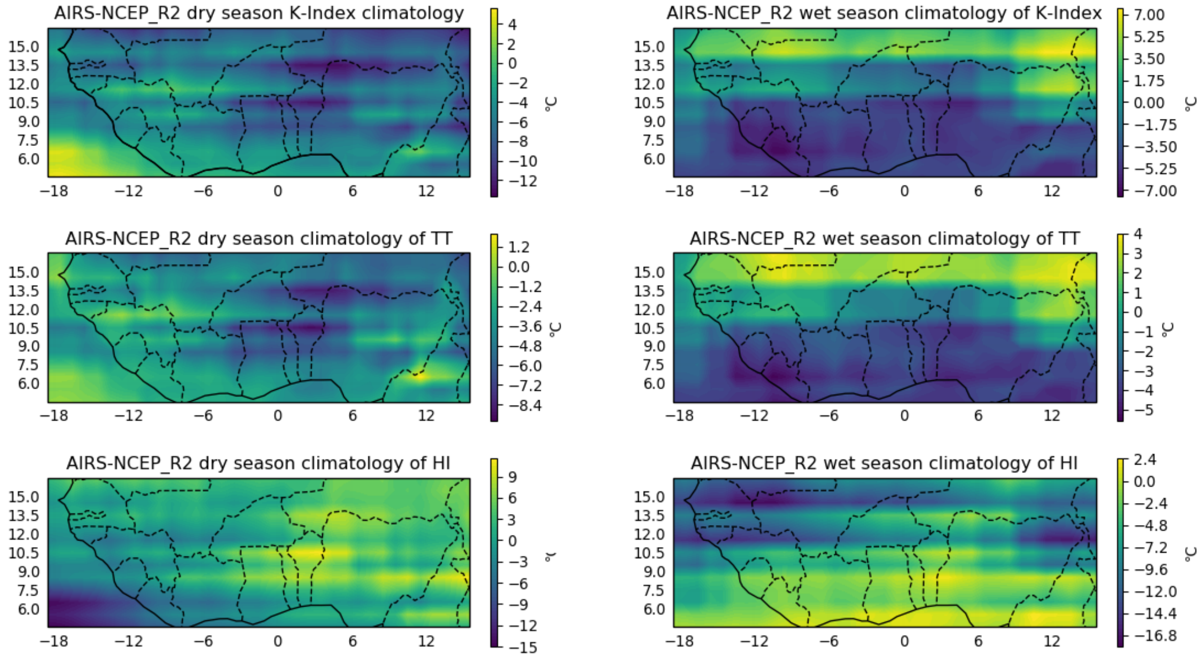

Figure 7. Difference in the index seasonal index climatology between AIRS and NCEP_R2 (AIRS-NCEP_R2). Dry season include months December, January and February whereas the wet season includes all other months.

due to the accuracy of AIRS in retrieving relative humidity profiles over the sea than coast and inland (Divakarla et al., 2006), resulting in a direct effect on the calculation of K-Index from AIRS datasets. The corresponding wet season climatology shows a high thunderstorm probability from NCEP_R2 analysis situated over inland Liberia ($<$ -7 °C). Few areas are found to have no difference in thunderstorm prediction over West Africa in the wet season from the K-Index (0 °C). A higher thunderstorm probability in AIRS is observed in the inland regions the vicinity of the Sahelian with over-estimated values reaching about 7 °C. In the dry season (Figure 7), the AIRS TT index over-estimates the rainfall activities by locating a hotspot ($>$ 1.2 °C difference) at the Nigeria-Cameroonian border. This was also captured by the K-Index however at a difference of $\approx$ 3 °C. It can be observed that the seasonal differences in AIRS and NCEP_R2 for the derivation of the TT index is relatively lower than the other indices. The wet season TT index likewise the K-index is also observed to have a higher rainfall likelihood (from AIRS) at the Sahelian region and no difference at the sudano-savanna region. In addition, the observation for the K and TT wet season indices show that the AIRS over-estimations have a latitudinal increase from the coast to further inland regions of West Africa (Figure 7). The intensity of over- and under-estimation of AIRS in the dry season HI is observed to be in complete opposite to the K-index dry season climatology. On the other hand, inland areas where AIRS obtained larger under-estimations in K-index corresponded to higher over-estimations in the HI for the dry season. Nonetheless, the western regions of West Africa was obtained relatively no difference in thunderstorm prediction for AIRS and NCEP_R2 in the dry season. For the wet season, HI differences although lower than the dry season, has AIRS over-predicting rainfall in most areas of the West African sub-region (Figure 7).

The seasonal comparison of the indices derived from AIRS and NCEP_R2 collocations with radiosonde calculated indices is given in Tables 3 and 4. A general observation was a better correlation between AIRS and RAOB calculated indices at the stations. The slight overestimation found in NCEP_R2 from Figure 5 is also observed in the extracted indices at

Table 3. Comparison of AIRS and NCEP_R2 derived stability indices in the dry season (December-February). Units of all indices in degree Celsius (°C)

Station	K-Index RAOB	AIRS	NCEP	TT index RAOB	AIRS	NCEP	HI RAOB	AIRS	NCEP
Abidjan	23.86	25.13	25.80	38.43	40.64	40.65	29.73	29.55	28.80
Cotonou	23.18	25.47	20.58	37.30	40.47	38.78	29.58	22.33	40.34
Ougadougou	-1.85	-9.37	9.44	21.81	13.50	27.78	77.31	95.89	63.57
Parakou	21.05	23.50	28.82	37.52	38.02	43.80	42.53	42.75	38.00
Tamale	-2.26	-0.66	21.88	27.97	30.53	46.05	76.75	72.46	45.61

the stations was also found to be higher than RAOB calculated indices. In the dry season, the coastal stations Abidjan and Cotonou had lower bias as compared to the RAOB, in the K-Index, TT index and the HI for both AIRS and NCEP_R2. The HI however has a larger difference for NCEP_R2 with the RAOB over Cotonou to suggest the low chance of thunderstorm formation at the coastal station. Over Ougadougou, the difference in K-Index between AIRS and RAOB was found to be low (-7.59 °C) as compared to RAOB and NCEP_R2 (11.29 °C). The TT index and HI revealed on the other hand obtained a higher bias between AIRS and RAOB (Table 3). The capability of AIRS in measuring the very low dry season humidity conditions over Ougadougou is observed to translate into the low TT and corresponding HI. The AIRS derived indices suggest virtually no probability for thunderstorm occurrence which is to be expected over the station during this period. Over Parakou there was a good agreement between RAOB and AIRS derived indices although NCEP_R2 was also not highly biased. The K-Index at Tamale agreed only in the AIRS (-0.66° C) and RAOB (-2.26° C) datasets with the NCEP_R2 over-estimating in both K-index and TT and underestimating in the HI (Table 3). But in general, the low probability of thunderstorm occurrence at these stations were well observed by the indices for the dry season.

The RAOB indices for the wet season at the stations is shown in Table 4. The derived indices for RAOB, AIRS and NCEP_R2 were in agreement with low biases. The humidity index also observed values which were below 30° C and supports the the increased chances of thunderstorm events as moisture is advected by the south-western winds towards these stations. Close agreement was found at the Accra station between ROAB and NCEP_R2 for George's K and TT indices. In most instances, AIRS and NCEP_R2 had a relatively perfect agreement for thunderstorm prediction. Furthermore, AIRS and NCEP_R2 marginally over-estimate the indices (K and TT indices) compared to RAOB and under-estimates the HI. But there exists a good correspondence between AIRS and RAOB HI over Accra and Kumasi.

4 Conclusions

Determination of a pre-convective environment for thunderstorm formation requires a long time-series of sounding data. Radiosonde observation offer the most accurate vertical profiles of temperature and relative humidity. However these observations are scarce in West Africa and hence the need to rely on suitable satellite products for convection assessment.

Table 4. Comparison of AIRS and NCEP_R2 derived stability indices in the wet season (March-November). Units of all indices in degree Celsius (°C)

Station	K-Index RAOB	AIRS	NCEP	TT index RAOB	AIRS	NCEP	HI RAOB	AIRS	NCEP
Abidjan	27.77	28.20	30.01	40.18	41.26	41.45	21.57	21.56	17.95
Accra	28.50	30.99	28.61	39.95	40.83	39.73	19.44	15.18	14.29
Cotonou	23.35	32.21	31.26	35.51	42.04	42.05	21.78	14.24	15.90
Kumasi	28.19	31.32	32.74	40.51	42.37	42.80	18.82	15.55	12.51
Ougadougou	22.72	31.80	33.57	37.45	45.27	46.36	28.90	22.78	23.74
Parakou	29.15	33.52	33.79	41.82	43.39	44.37	21.44	14.24	15.64
Tamale	29.78	32.48	32.36	42.76	45.40	46.99	23.97	23.21	17.24

The Atmospheric InfraRed Sounder on-board the AQUA satellite provides atmospheric sounding information twice daily, which may be used as a reliable substitute for RAOB observation globally. The study assessed the performance of the AIRS IR-Only level 3 standard retrieval version 6 and for context, NCEP_R2 vertical temperature and relative humidity profiles for some select AMMA and DACCIWA radiosonde observation stations in West Africa within spatio-temporal collocation radius of 100 km and ±3 hours for AIRS and NCEP_R2. The performance of AIRS vertical profiles for diurnal, seasonal, cloud and cloud-free analyses as well as with collocated NCEP_R2 profiles were assessed. Finally seasonal variation of three thunderstorm convective indices (K-Index, TT index and HI) for each station was computed and compared for RAOB, AIRS and NCEP_R2.
The diurnal temperature profile reveals lower biases however with corresponding higher RMSD above the AIRS mission goal of ±1 °K. AIRS temperature RMSD show higher values at the coast as compared to inland regions, possibly due to complications in surface emissivity, skin temperature and the diurnal sea and land breeze effect which is strongest along the coast. The reverse of the temperature RMSD however is observed to occur at night. The relative humidity on the other hand, was found to be more accurate for the descending pass than ascending for all zones with the coastal stations dominating in all passes. On the seasonal timescale, the temperature bias for the dry season is pre-dominantly cold. The corresponding RMSD were also higher and deviated towards the inland wet season profile. The coastal dry season was the least deviated, albeit, all zonal deviations were higher (≈1.0 - 5 °K). Inland wet season RH profile was the most biased (cold) whereas the RMSD showed satisfactory performance at all level tropospheric levels for all zones and seasons. Cloudy conditions were found to have no significant effect on the RH retrievals by AIRS as the bias and RMSD between cloudy and non-cloudy days were found to have marginal differences and both achieving the AIRS accuracy goal of $< 20\%$ and 50% for lower and upper troposphere respectively. The temperature retrievals however are better on cloud-free than cloudy days. Comparison of the temperature and RH retrievals of AIRS with NCEP_R2 reveal AIRS to be a better substitute for RAOB vertical profiles at the coast and inland. Finally, the seasonal derived thunderstorm indices for AIRS and NCEP_R2 showed that both datasets can be utilised for the occurrence and non-occurrence of thunderstorms in the wet and dry seasons though NCEP_R2 generally over-estimates the thunderstorm probability. Comparing the derived indices of AIRS and NCEP_R2 with RAOB indices at the seven stations also show a higher agreement for all seasons.
In general, the performance of AIRS at these West African stations has been satisfactory for the temperature (although with slight over-estimations) and the RH. Based on the

performance of AIRS for the derivation of thunderstorm convective instability indices, it is proposed to be used further for the determining the probability of convection initiation over West Africa under the GCRF African SWIFT project by focusing on the statistical analysis of thunderstorm convective indices over the region.

Acknowledgments

The authors would like to acknowledge the support GCRF African SWIFT project for funding this research. We appreciate Douglas Parker for his contribution to this study. We acknowledge the AMMA and NCAS for providing us with the AMMA and DACCIWA radiosonde datasets respectively. Based on an French initiative, AMMA was built by an international scientific group and is currently funded by a large number of agencies, especially from France, UK, US and Africa. It has been the beneficiary of a major financial contribution from the European Community's Sixth Framework Research Programme. Detailed information on scientific coordination and funding is available on the AMMA International web site `http://www.amma-international.org`'. Finally we acknowledge the Goddard Earth Sciences Data and Information Services Center for making the AIRS datasets available online at `http://disc.sci.gsfc.nasa.gov/AIRS/data_access.shtml`. We also acknowledge the physical sciences division of hte Earth System Research Laboratory for making the NCEP-DOE Reanalysis 2 dataset available online at `https://www.esrl.noaa.gov/psd/`.

References

Amekudzi, L. K., Yamba, E. I., Preko, K., Asare, E. O., Aryee, J., Baidu, M., & Codjoe, S. N. (2015). Variabilities in rainfall onset, cessation and length of rainy season for the various agro-ecological zones of ghana. *Climate*, *3*(2), 416–434.

Aumann, H. H., Chahine, M. T., Gautier, C., Goldberg, M. D., Kalnay, E., McMillin, L. M., ... others (2003). Airs/amsu/hsb on the aqua mission: Design, science objectives, data products, and processing systems. *IEEE Transactions on Geoscience and Remote Sensing*, *41*(2), 253–264.

Baidu, M., Amekudzi, L. K., Aryee, J. N., & Annor, T. (2017). Assessment of long-term spatio-temporal rainfall variability over ghana using wavelet analysis. *Climate*, *5*(2), 30.

Bayat, A., & Maleki, S. M. (2018). Comparison of precipitable water vapor derived from airs and spm measurements and its correlation with surface temperature of 29 synoptic stations over iran. *Journal of Atmospheric and Solar-Terrestrial Physics*.

Boylan, P., Wang, J., Cohn, S. A., Fetzer, E., Maddy, E. S., & Wong, S. (2015). Validation of airs version 6 temperature profiles and surface-based inversions over antarctica using concordiasi dropsonde data. *Journal of Geophysical Research: Atmospheres*, *120*(3), 992–1007.

Chen, M., Wang, Y., Gao, F., & Xiao, X. (2014). Diurnal evolution and distribution of warm-season convective storms in different prevailing wind regimes over contiguous north china. *Journal of Geophysical Research: Atmospheres*, *119*(6), 2742–2763.

Diao, M., Jumbam, L., Sheffield, J., Wood, E. F., & Zondlo, M. A. (2013). Validation of airs/amsu-a water vapor and temperature data with in situ aircraft observations from the surface to ut/ls from 87 n–67 s. *Journal of Geophysical Research: Atmospheres*, *118*(12), 6816–6836.

Divakarla, M. G., Barnet, C. D., Goldberg, M. D., McMillin, L. M., Maddy, E., Wolf, W., ... Liu, X. (2006). Validation of atmospheric infrared sounder temperature and water vapor retrievals with matched radiosonde measurements and forecasts. *Journal of Geophysical Research: Atmospheres*, *111*(D9).

Ferguson, C., & Wood, E. (2010). An evaluation of satellie remote sensing data products for land surface hydrology: Atmospheric Infrared Sounder. *Journal of Hydrometeorology*, *11*, 1234–1261.

Ferguson, C., & Wood, E. (2011). Observed land-atmosphere coupling from satellite remote sensing and reanalysis. *Journal of Hydrometeorology*, *12*(6), 1221–1254.

Flores, F., Rondanelli, R., Díaz, M., Querel, R., Mundnich, K., Herrera, L. A., … Carricajo, T. (2013). The life cycle of a radiosonde. *Bulletin of the American Meteorological Society*, *94*(2), 187–198.

George, J. (1960). Weather forecasting for aeronautics. *Academic Press*, 409-415.

He, X., Kim, H., Kirstetter, P.-E., Yoshimura, K., Chang, E.-C., Ferguson, C. R., … Oki, T. (2015). The diurnal cycle of precipitation in regional spectral model simulations over west africa: Sensitivities to resolution and cumulus schemes. *Weather and Forecasting*, *30*(2), 424–445.

Jacovides, C., & Yonetani, T. (1990). An evaluation of stability indices for thunderstorm prediction in greater cyprus. *Weather and forecasting*, *5*(4), 559–569.

Kanamitsu, M., Ebisuzaki, W., Woollen, J., Yang, S.-K., Hnilo, J., Fiorino, M., & Potter, G. (2002). Ncep–doe amip-ii reanalysis (r-2). *Bulletin of the American Meteorological Society*, *83*(11), 1631–1644.

Knippertz, P., Fink, A. H., Deroubaix, A., Morris, E., Tocquer, F., Evans, M. J., … others (2017). A meteorological and chemical overview of the dacciwa field campaign in west africa in june–july 2016. *Atmospheric Chemistry and Physics*, *17*(17), 10893–10918.

Liang, C., Eldering, A., Gettelman, A., Tian, B., Wong, S., Fetzer, E., & Liou, K. (2011). Record of tropical interannual variability of temperature and water vapor from a combined airs-mls data set. *Journal of Geophysical Research: Atmospheres*, *116*(D6).

Madhulatha, A., Rajeevan, M., Venkat Ratnam, M., Bhate, J., & Naidu, C. (2013). Nowcasting severe convective activity over southeast india using ground-based microwave radiometer observations. *Journal of Geophysical Research: Atmospheres*, *118*(1), 1–13.

Marinaki, A., Spiliotopoulos, M., & Michalopoulou, H. (2006). Evaluation of atmospheric instability indices in greece. *Advances in Geosciences*, *7*, 131–135.

McMillin, L. M., Zhao, J., Rama Varma Raja, M., Gutman, S. I., & Yoe, J. G. (2007). Radiosonde humidity corrections and potential atmospheric infrared sounder moisture accuracy. *Journal of Geophysical Research: Atmospheres*, *112*(D13).

Mears, C. A., Wang, J., Smith, D., & Wentz, F. J. (2015). Intercomparison of total precipitable water measurements made by satellite-borne microwave radiometers and ground-based gps instruments. *Journal of Geophysical Research: Atmospheres*, *120*(6), 2492–2504.

Miller, R. C. (1975). *Notes on analysis and severe-storm forecasting procedures of the air force global weather central* (Vol. 200). AWS.

Milstein, A. B., & Blackwell, W. J. (2016). Neural network temperature and moisture retrieval algorithm validation for airs/amsu and cris/atms. *Journal of Geophysical Research: Atmospheres*, *121*(4), 1414–1430.

Olsen, E. T. (2016). Airs version 6.1.1 processing files description. *Goddard Space Flight Center, NASA, Jet Propulsion Laboratory, California Institute of Technology, Pasadena, CA*.

Olsen, E. T., Manning, E., Licata, S., Blaisdell, J., Iredell, L., & J, S. (2017). Airs/amsu/hsb version 6 data release user guide. *Goddard Space Flight Center, NASA, Jet Propulsion Laboratory, California Institute of Technology, Pasadena, CA*.

Parker, D. J. (2017). *Meteorology of tropical west africa: The forecasters' handbook*. John Wiley & Sons.

Peppler, R. A. (1988). *A review of statics stability indices and related thermody-*

namic parameters. (Tech. Rep.). Illinois State Water Survey.

Pfahl, S., & Niedermann, N. (2011). Daily covariations in near-surface relative humidity and temperature over the ocean. *Journal of Geophysical Research: Atmospheres*, *116*(D19).

Prasad, A. K., & Singh, R. P. (2009). Validation of modis terra, airs, ncep/doe amip-ii reanalysis-2, and aeronet sun photometer derived integrated precipitable water vapor using ground-based gps receivers over india. *Journal of Geophysical Research: Atmospheres*, *114*(D5).

Quaas, J. (2012). Evaluating the critical relative humidity as a measure of subgrid-scale variability of humidity in general circulation model cloud cover parameterizations using satellite data. *Journal of Geophysical Research: Atmospheres*, *117*(D9).

Reale, A., Tilley, F., Ferguson, M., & Allegrino, A. (2008). Noaa operational sounding products for advanced tovs. *International Journal of Remote Sensing*, *29*(16), 4615–4651.

Redelsperger, J.-L., Thorncroft, C. D., Diedhiou, A., Lebel, T., Parker, D. J., & Polcher, J. (2006). African monsoon multidisciplinary analysis: An international research project and field campaign. *Bulletin of the American Meteorological Society*, *87*(12), 1739–1746.

Singh, T., Mittal, R., & Shukla, M. V. (2017). Validation of insat-3d temperature and moisture sounding retrievals using matched radiosonde measurements. *International journal of remote sensing*, *38*(11), 3333–3355.

Susskind, J. (2006). Improved soundings and error estimates using airs/amsu data. In *Algorithms and technologies for multispectral, hyperspectral, and ultraspectral imagery xii* (Vol. 6233, p. 623319).

Susskind, J. (2007). Recent theoretical advances in analysis of airs/amsu sounding data. In *Algorithms and technologies for multispectral, hyperspectral, and ultraspectral imagery xiii* (Vol. 6565, p. 65651H).

Susskind, J., Barnet, C. D., & Blaisdell, J. M. (2003). Retrieval of atmospheric and surface parameters from airs/amsu/hsb data in the presence of clouds. *IEEE Transactions on Geoscience and Remote Sensing*, *41*(2), 390–409.

Susskind, J., Blaisdell, J. M., Iredell, L., & Keita, F. (2011). Improved temperature sounding and quality control methodology using airs/amsu data: The airs science team version 5 retrieval algorithm. *IEEE Transactions on Geoscience and Remote Sensing*, *49*(3), 883–907.

Taylor, C. M., Belušić, D., Guichard, F., Parker, D. J., Vischel, T., Bock, O., … Panthou, G. (2017). Frequency of extreme sahelian storms tripled since 1982 in satellite observations. *Nature*, *544*(7651), 475.

Wang, Y., Zhou, D., Bunde, A., & Havlin, S. (2016). Testing reanalysis data sets in antarctica: Trends, persistence properties, and trend significance. *Journal of Geophysical Research: Atmospheres*, *121*(21).

Wong, S., Fetzer, E. J., Schreier, M., Manipon, G., Fishbein, E. F., Kahn, B. H., … Irion, F. W. (2015). Cloud-induced uncertainties in airs and ecmwf temperature and specific humidity. *Journal of Geophysical Research: Atmospheres*, *120*(5), 1880–1901.

Xuebao, W., Jun, L., Wenjian, Z., & Fang, W. (2005). Atmospheric profile retrieval with airs data and validation at the arm cart site. *Advances in Atmospheric Sciences*, *22*(5), 647–654.